

Effect of Bayesian penalty likelihood algorithm on 18F-FDG PET/CT image of lymphoma

Yongtao Wang^{a,*}, Lejun Lin^{a,*}, Wei Quan^b, Jinyu Li^a and Weilong Li^a

Objective Recently, a new Bayesian penalty likelihood (BPL) reconstruction algorithm has been applied in PET, which is expected to provide better image resolution than the widely used ordered subset expectation maximization (OSEM). The purpose of this study is to compare the differences between these two algorithms in terms of image quality and effects on clinical diagnostics and quantification of lymphoma.

Methods A total of 246 FDG-positive lesions in 70 patients with lymphoma were retrospectively analyzed by using BPL and OSEM + time-of-flight + point spread function algorithms. Visual analysis was used to evaluate the effects of different reconstruction algorithms on clinical image quality and diagnostic certainty. Quantitative analysis was used to compare the differences between pathology and lesion size.

Results There were significant differences in lesion-related SUVmax, total-lesion-glycolysis (TLG), and signal-to-background ratio (SBR) ($P < 0.01$). The variation Δ SUVmax% and Δ SBR% caused by the two reconstruction algorithms were negatively correlated with tumor diameter, while Δ MTV% and Δ TLG% were positively correlated with tumor diameter. In the grouped analysis based on pathology, there were significant differences in lesion SUVmax, lesion SUVmean, and SBR. In non-Hodgkin's lymphoma (diffuse large B cells and follicular lymphoma), diversities were significantly found in SUVmax, SUVmean, SBR, and TLG of the lesions

($P < 0.05$). According to the grouped analysis based on lesion size, for lesions smaller than 1 cm and 2 cm, there was a significant difference in SUVmean, SUVmax, SBR, and MTV, but not in lesions larger than or equal to 2 cm ($P > 0.05$), and the liver background SUVmean ($P > 0.05$) remained unchanged.

Conclusion BPL reconstruction algorithm could effectively improve clinical image quality and diagnostic certainty. In quantitative analysis, there were no significant differences among different pathological groups, but there were significant diversities in lesion sizes. Especially for small lesions, lesion SUVmax increased and SBR was significantly improved, which may better assist in the diagnosis of small lesions of lymphoma. *Nucl Med Commun* 43: 284–291 Copyright © 2021 The Author(s). Published by Wolters Kluwer Health, Inc.

Nuclear Medicine Communications 2022, 43:284–291

Keywords: Bayesian penalty likelihood, FDG, lymphoma, PET, SUV

Departments of ^aNuclear Medicine and ^bMedical Imaging, The Affiliated Yantai Yuhuangding Hospital of Qingdao University, Zhifu District, Yantai, Shandong Province, People's Republic of China

Correspondence to Weilong Li, MD, Department of Nuclear Medicine, The Affiliated Yantai Yuhuangding Hospital of Qingdao University, Yudong Road No. 20, Zhifu District, Yantai, Shandong Province 264000, People's Republic of China
Tel: +86 15216387901; e-mail: 389952020@qq.com

*Yongtao Wang and Lejun Lin contributed equally to the writing of this article.

Received 5 August 2021 Accepted 16 November 2021

Introduction

Background: PET and 18F-deoxyglucose (18F-FDG) are widely used in oncology diagnosis, staging, disease recurrence, and patient management. Lymphoma, in particular, clinically relies on PET/computed tomography (CT) to quantify the overall disease burden and evaluate treatment response, as well as treatment guidance [1]. At the end of the relevant course of treatment, PET/CT can be used to evaluate the effectiveness of treatment and to determine whether there are residual signs of the tumor [2]. Especially for small lesions, the detection rate was limited by partial volume effect (PVE) and traditional reconstruction techniques that cannot achieve complete

convergence, which may cause a lower signal-to-noise ratio and poor visual detectability. In the past decade, PET technology has made some progress, including new hardware functions, such as time-of-flight (TOF) acquisition [3] and advanced image reconstruction methods of point spread function (PSF) [4], so that PET images have been substantially improved. The detectability of lesions and standardized uptake value (SUV) of lymph nodes of ordered subset expectation maximization (OSEM) reconstruction with TOF and PSF were better than those of conventional OSEM reconstruction [5]. In recent years, GE Healthcare (Milwaukee, USA) proposed a new iterative image reconstruction algorithm called Q.Clear [6], which combines the Bayesian penalty likelihood (BPL) algorithm. Q.Clear considers all aspects of the image reconstruction process, including PSF modeling and an innovative penalty factor [7], so that the algorithm can achieve complete convergence [8]. The penalty function

This is an open-access article distributed under the terms of the Creative Commons Attribution-Non Commercial-No Derivatives License 4.0 (CCBY-NC-ND), where it is permissible to download and share the work provided it is properly cited. The work cannot be changed in any way or used commercially without permission from the journal.

is controlled by a penalty factor called β , which is the only variable in the algorithm that can be modified by the operator. Therefore, compared with OSEM reconstruction, the SUV value obtained by the BPL algorithm is more accurate than that obtained by OSEM, and the image resolution is higher, which has great potential in enhancing 18F-FDG PET image quality [9]. The purpose of this study is to compare the traditional OSEM + TOF + PSF reconstruction algorithm with the latest BPL algorithm and to investigate their effects on the image quality, clinical diagnosis, and quantitative analysis of lymphoma.

Materials and methods

Clinical data

The data of consecutive cases examined by 18F-FDG PET/CT in the PET/CT center of our hospital from March 2020 to December 2020 were retrospectively analyzed. There were 42 males and 28 females. The average age was 51.67 ± 16.09 -years old (range 19–83 years), and the average BMI was 24.58 ± 4.03 (range: 14.88–33.91). There were eight cases of Hodgkin's lymphoma and 62 cases of non-Hodgkin's lymphoma, including 31 cases of diffuse large B cells, 18 cases of follicular lymphoma, and 13 cases of other types.

18F-FDG PET/CT image acquisition and analysis

The subjects were under normal fasting conditions for more than 6 hours and their blood glucose was less than or equal to 11.11 mmol/L. 18F-FDG was injected with a dose of 3.67 ± 0.01 mol (3.65–3.69 g) MBq/kg. The acquisition began 60 mins after injection using Discovery 710Clarity PET/CT (GE Healthcare, Milwaukee, USA). Body PET scans were performed from the base of the skull to the upper part of the femur. PET collection parameters were 1.5 min/bed, free-breathing, matrix 192×192 . CT collection parameters were layer thickness, 3.75 mm, voltage 120 kVp, auto mA:30~180. PET reconstruction used OSEM (three iteration/24 subsets, 6.4 mm Gaussian filter) + TOF + Sharp IR (PSF), and BPL mode ($\beta = 570$). BPL is Q.Clear by GE Healthcare, Milwaukee, USA) and β is the regularization factor, of which the function is to regulate the regularization effect [11].

The data obtained were divided into two groups of different reconstruction algorithms (OSEM + TOF + PSF and BPL), and the differences in metabolic parameters were compared. Using pathology as the distinctive criteria, data were then divided into four subgroups: Hodgkin, diffuse large cell B, follicular, and others. Finally, data were divided into three groups of different lesion sizes: long-axis diameter less than 1 cm, 1–2 cm, or more than 2 cm. The reconstructed PET/CT images were processed by the AW4.7 workstation (GE Healthcare, Milwaukee, USA). The long-axis diameter (D) of the lesion on the fused image was measured. Lesions were delineated according to the 42% threshold method, and the normal background

tissue was selected using spherical volumes-of-interest (VOIs), with a diameter of 1 cm in the right posterior lobe of the liver, while avoiding the location of tumor focus, inflammation, hyperplasia, and other lesions. The metabolic parameters of VOIs, including focus SUV_{mean}, SUV_{max}, metabolic tumor volume (MTV), and calculate total-lesion-glycolysis (TLG), liver SUV_{mean}-liver and tissue signal-to-back ratio [signal-to-background ratio (SBR)] to evaluate the image quality of PET/CT were recorded. The change rates of SUV_{max}, SBR, MTV, and TLG in BPL and non-BPL groups were calculated at the same time, such as $\Delta \text{SBR}\% = \text{SBR change rate}\% = (\text{SBR}_{\text{BPL}} - \text{SBR}_{\text{non-BPL}}) \times 100\% / \text{SBR}_{\text{non-BPL}}$.

Two experienced nuclear medicine doctors (with 10 and 15 years of experience in nuclear medicine, respectively) were asked to evaluate the image quality of the 70 positive lymphoma lesions on PET images reconstructed randomly and sequentially by OSEM and BPL methods, using a 4-point scale:

- 1 = Poor, the lesions were not visible, and the degree of 18F-FDG uptake was below the background.
- 2 = Moderate, the degree of 18F-FDG uptake is higher than that of background, but it is difficult to distinguish from noise.
- 3 = Good, the uptake of 18F-FDG is higher than that of the background and can be distinguished from noise.
- 4 = Excellent, good significance, higher 18F-FDG uptake than the background, can be distinguished from noise, and the perimeter of focus can be defined.

At the same time, a 4-point rating scale was also used to evaluate the certainty of image quality for diagnosis:

- 1 = Poor, uncertainty, image was not helpful for diagnosis.
- 2 = Moderate, lesions were shown, but the diagnostic accuracy was not strong.
- 3 = Good, good certainty, lesions were clearly shown and helped for the clinical diagnosis.
- 4 = Excellent, high certainty of diagnosis.

The evaluation of the two observers was conducted independently, did not know the clinical information and PET reconstruction methods, and was distinguished only by clinical experience.

Statistical analysis

All the data are expressed following the mean \pm SD, and statistical analysis is carried out by using the SPSS22.0 software (IBM Co., New York, USA). The image quality and diagnostic score were compared by nonparametric rank-sum test. The metabolic parameters of different reconstruction techniques, pathological subgroups, and lesion size groups were compared by the *t*-test and one-way ANOVA. The relationship between the change rate of metabolic parameters and diameter produced by the two reconstruction methods was analyzed by Pearson

correlation analysis. The difference was statistically significant when $P < 0.05$.

Results

The characteristics of all patients and reconstructed data are shown in Table 1. In this study, 70 patients included 246 FDG-positive lesions, with an average size of 1.56 ± 0.31 cm.

Visual analysis results

The consistency intraclass correlation coefficient of the two observers was 0.706 ($P < 0.001$). The distribution of image quality and diagnostic certainty was shown in Fig. 1. About 17.61% and 21.83% of the lesions can not be visualized or provide effective clinical diagnostic information on the images of non-BPL reconstruction algorithms, while the lesions using the BPL reconstruction algorithm accounted for 94.37% and 63.38%, respectively. These differences were statistically significant ($P < 0.001$) (Fig. 2).

The results of quantitative analysis between different reconstruction techniques groups

The statistical results of metabolic parameters between the two groups according to different reconstruction parameters are shown in Table 2. There was no significant difference in background SUVmean uptake and lesion metabolic volume MTV between the two groups using the BPL algorithm and OSEM + TOF + PSF algorithm, but there was a significant difference in lesion-related SUVmax, TLG, and SBR between the two groups ($P < 0.05$). The results of correlation analysis between the change of metabolic parameters and lesion diameter were shown in Table 3. Δ SUVmax% and Δ SBR% were negatively correlated with tumor diameter, while Δ MTV% and Δ TLG% were positively correlated with tumor diameter.

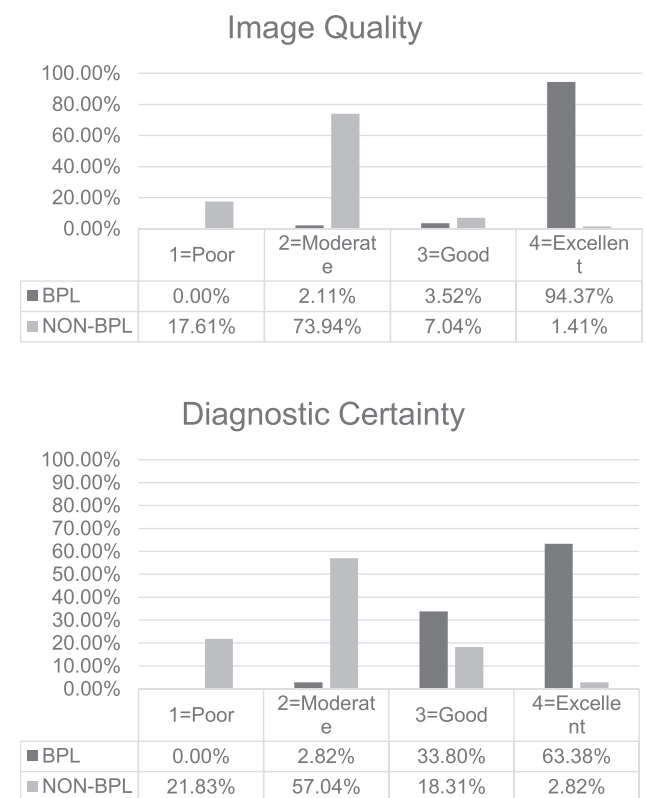
Comparison of metabolic parameters among different pathological groups

The data distribution and paired t -test comparison results were shown in Table 4 and Fig. 3. In the first group of Hodgkin lymphoma, there was no significant difference in liver background SUVmean, MTV, TLG, but diversities were found in lesion SUVmax, SUVmean, and SBR between the two reconstruction algorithms. In the second group and the third group of lesions with non-Hodgkin's lymphoma (the pathological types were diffuse large B and follicular type, respectively), there was no significant difference in liver background SUVmean, MTV between the two reconstruction algorithms, but diversities were found in lesion SUVmax, SUVmean, SBR, and TLG. In the fourth group (other pathology), significant differences were found in lesion SUVmax and liver background SUVmean. There was no significant difference in Δ SUVmax%, Δ SBR%, Δ MTV%, Δ TLG% among different pathological groups.

Table 1 Basic information of the examinee

Clinical info	Clinical data
Gender female/male (%)	28 (40%)/42 (60%)
Age (years-old)	51.67 ± 16.09 (19–83)
BMI (kg/m^2)	24.58 ± 4.03 (14.88–33.91)
The dose of 18F-FDG (MBq/kg)	3.67 ± 0.01 (3.65–3.69)
Glucose (mmol/l)	5.86 ± 1.03 (4.7–11)
Diagnostic (Pathology)	
Hodgkin (%)	8 (11.43%)
Non-Hodgkin (%)	62 (88.57%)
Diffuse large B cells (%)	31 (44.29%)
Follicular lymphoma (%)	18 (25.71%)
others(%)	13 (18.57%)

Fig. 1

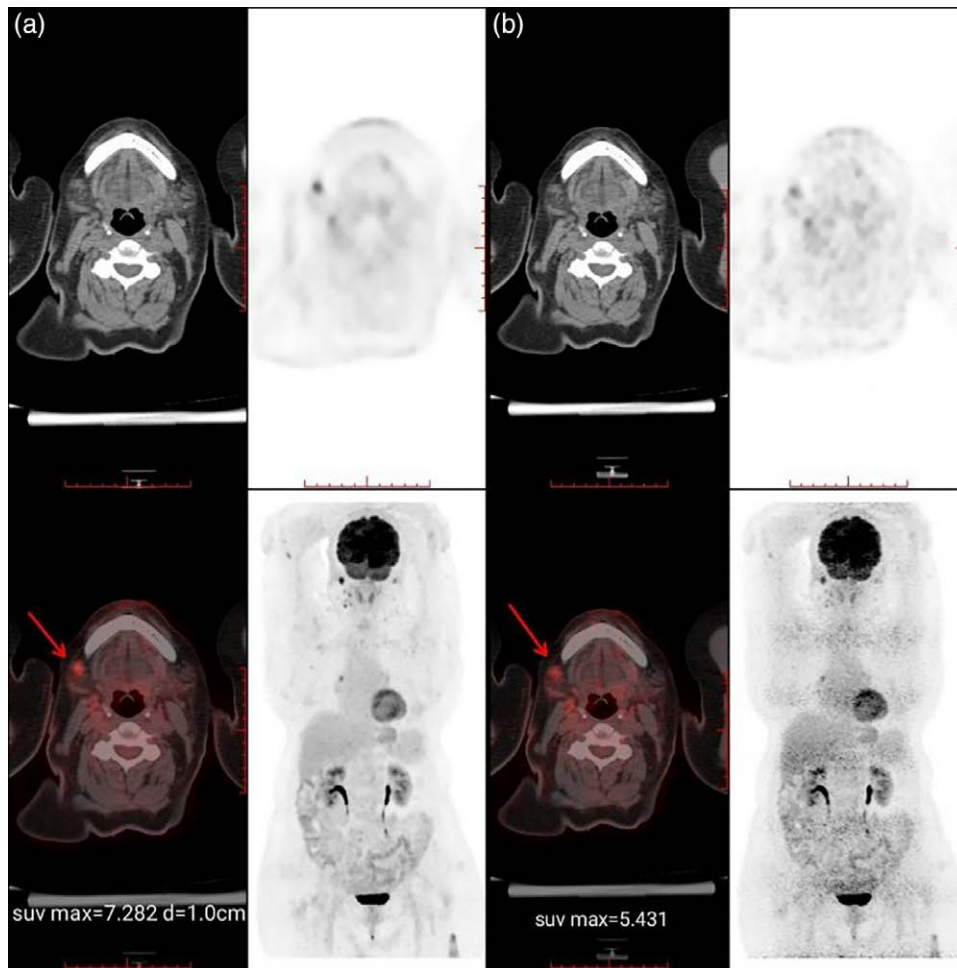


Visual scores of clinical image quality and diagnostic certainty using Bayesian penalty likelihood (BPL) and non-BPL algorithms.

Comparison of metabolic parameters with different lesion sizes

For lesions smaller than 2 cm, there was a significant difference in SUVmean, SUVmax, SBR, and MTV between BPL and OSEM + TOF + PSF reconstruction algorithms, but there was no significant difference in SUVmean, SUVmax, SBR, and MTV in lesions larger than or equal to 2 cm ($P > 0.05$). However, there was no significant difference in liver background SUVmean among the three groups ($P > 0.05$). TLG was only affected by the reconstruction algorithm in the lesions smaller than 1 cm ($P < 0.05$) and larger than 2 cm ($P < 0.01$) (Table 5).

Fig. 2



The clinical case showed a 57-year-old female with non-Hodgkin's lymphoma (B-cell type) in August 2020. Before treatment, systemic PET-CT examination was performed to evaluate the image reconstructed by the following: (a) using BPL, the right maxillofacial lymph node focus SUVmax = 7.28, clinician scored 4 points for image quality and diagnostic accuracy. (b) using OSEM + PSF + TOF, the right maxillofacial lymph node lesion SUVmax = 5.43. Clinicians scored 2 points for image quality and 2 points for diagnostic accuracy. BPL, Bayesian penalty likelihood; CT, computed tomography; OSEM, ordered subset expectation maximization; PSF, point spread function; SUV, standardized uptake value; TOF, time-of-flight.

Discussion

In the past few years, many reconstruction algorithms have been introduced to reduce errors and artifacts, which affect the quality of clinical images, as well as the accuracy and repeatability of quantitative parameters SUV. At present, the clinical standard for PET image reconstruction is an iterative algorithm, mainly an OSEM algorithm, which has a tradeoff between the number of subsets and image quality: each subset contains less tomography and statistical information, so noise and artifacts will increase [10]. To achieve the complete convergence of the image in the process of reconstruction, multiple iterations are needed; however, with the increase of the number of iterations, the background noise will also increase. On the contrary, because the reconstruction of the image is

limited to reducing noise, it can not achieve complete convergence, thus reducing the accuracy and quality of the PET image. With the development of technology, the technology of TOF and PSF is gradually improved, and the spatial resolution is partially compensated. TOF mainly improves the SNR through temporal resolution [11] but does not affect the standardized uptake value (SUV) [5], while PSF mainly improves the spatial resolution of reconstruction [12]. In clinical studies, SUVmax increases by more than 30% [13]. Both TOF and PSF are beneficial to the tradeoff between (CR) and SNR, but all these reconstruction methods (OSEM + TOF + PSF) have a limitation in principle, that is, to obtain sufficient contrast recovery by increasing the number of iterations/subsets will be at the cost of reducing SNR.

The BPL reconstruction algorithm considers all aspects of the image reconstruction process, including PSF modeling and an innovative penalty factor. The penalty factor is a function, which is given by the value difference between adjacent voxels and the sum of them. As a noise suppression, the algorithm achieves complete convergence and provides a high SNR for the image. In each iteration, compared with voxels with higher noise, voxels with smaller changes between adjacent voxels are slightly advantageous. BPL can regulate the image through the penalty factor β , and the selection of β can affect the comparison results between different algorithms. Reynés-Llompарт *et al.* conducted a model test using GE Discovery IQ PET/CT [14]. Under the NEMA NU-2012 standard, it was found that compared with PSF or OSEM (both without TOF), the CNR of

BPL reconstruction is improved ($\beta = 350$). Lindström *et al.* [15], reported that compared with OSEM, BPL had higher CNR with $\beta = 400$ –533 and poorer CNR with $\beta < 300$. In the study of Rogasch *et al.* [16], the tradeoff between CNR and SNR was the best when β was 300–450. While when $\beta = 150$, the SNR of the BPL reconstructed image was low, but the CRpeak of the sphere was not significantly improved. In clinical studies, such as the trial of Kurita *et al.* [17], it has been proved that BPL reconstruction was superior to OSEM + TOF + PSF reconstruction in the detection of small pulmonary nodules in patients with suspected primary and metastatic lung cancer. Compared with OSEM reconstruction, the observer chose BPL reconstruction as the preferred reconstruction for image evaluation, and the “intermediate” beta of 600 seems to be the ideal value for the evaluation of lung tumors in most cases. The beta selection in our experiment was 570, which was based on the previous trial and has been confirmed by clinicians. And there were also many studies on the improvement of the visibility of lung lesions by BPL. Howard *et al.* [18] compared BPL reconstruction with OSEM. They studied 32 nodules with an average lesion diameter of 8 mm (range 2–18 mm) in 29 patients and found that BPL reconstruction significantly improved the significance of the lesions. In another study by Teoh *et al.* [19], BPL reconstruction led to a significant increase in the maximum survival time (average 5.3–8.1, $P < 0.0001$), and the average percentage of SURVAMax in pulmonary nodules less than 1 cm (73%) was significantly higher than that in larger nodules (42%). Our current study showed that compared with OSEM + TOF + PSF reconstruction, the BPL method ($\beta = 570$) can improve the diagnostic accuracy, SUVmax, SBR, and MTV of lymph nodes of less than 2 cm, and had no impact on SUVmax of lesions that were larger than 2 cm. This was similar to some of the previous literature conclusions.

Table 2 Statistical results of metabolic parameters between two groups with different reconstruction parameters

Quantitative parameter	BPL	Non-BPL	P-value
Lesion SUVmax	15.25 ± 10.17	12.97 ± 7.87	0.000
Lesion MTV	4.18 ± 7.10	4.29 ± 6.37	0.273
Lesion TLG	43.00 ± 104.58	39.36 ± 93.41	0.000
Background liver SUVmean	2.52 ± 0.27	2.51 ± 0.30	0.558
SBR	6.02 ± 4.13	5.14 ± 3.54	0.000

BPL, Bayesian penalty likelihood; MTV, metabolic tumor volume; SBR, signal-to-background ratio; SUV, standardized uptake value; TLG, total-lesion-glycolysis.

Table 3 Correlation analysis between the change of metabolic parameters and the diameter of lesions

Pearson	Diameter (1.56 ± 1.22)	P-value
Δ SUVmax% (16.92% ± 29.12%)	−0.187	0.003
Δ SBR% (19.30% ± 30.92%)	−0.177	0.005
Δ MTV% (30.31% ± 85.55%)	0.138	0.031
Δ TLG% (6.6020% ± 68.80%)	0.13	0.04

MTV, metabolic tumor volume; SBR, signal-to-background ratio; SUV, standardized uptake value; TLG, total-lesion-glycolysis.

Table 4 Results of metabolic parameters among different pathological groups

	1 = Hodgkin	2 = Diffuse large B	3 = Follicular	4 = Others
Nodules (number)	59	102	69	16
Diameter (cm)	1.58 ± 1.20	1.72 ± 1.59	1.46 ± 0.51	0.91 ± 0.35
SUVmax-BPL	14.10 ± 7.07	17.92 ± 13.04	13.39 ± 7.29	10.71 ± 4.99
SUVmean-BPL	8.75 ± 4.62	11.77 ± 9.47	8.59 ± 5.02	6.80 ± 3.58
MTV-BPL	6.53 ± 12.79	3.72 ± 4.13	3.37 ± 3.06	1.73 ± 1.61
Liver SUV ^{mean} -BPL	2.46 ± 0.36	2.56 ± 0.38	2.53 ± 0.54	2.47 ± 0.42
TLG-BPL	75.61 ± 192.20	41.40 ± 61.94	25.16 ± 25.87	9.81 ± 8.70
SBR-BPL	5.74 ± 3.18	7.18 ± 5.19	5.69 ± 3.71	4.21 ± 1.44
SUVmax-non BPL	12.07 ± 6.32	14.88 ± 9.57	11.90 ± 6.43	8.70 ± 2.26
SUVmean-non BPL	7.11 ± 3.58	9.03 ± 5.96	7.21 ± 4.06	5.21 ± 1.42
MTV-non BPL	6.67 ± 11.38	3.82 ± 3.63	3.57 ± 3.05	1.67 ± 1.24
Liver SUV ^{mean} -non BPL	2.50 ± 0.38	2.54 ± 0.46	2.55 ± 0.55	2.26 ± 0.30
TLG-non BPL	68.06 ± 172.09	37.92 ± 54.39	23.99 ± 24.35	8.97 ± 8.30
SBR-non BPL	4.97 ± 2.68	6.05 ± 4.15	4.99 ± 3.28	3.83 ± 0.80
Δ SUVmax%	18.68% ± 21.93%	18.56% ± 36.71%	12.83% ± 18.59%	20.20% ± 34.35%
Δ SBR%	19.03% ± 27.96%	20.15% ± 38.84%	14.41% ± 23.98%	10.15% ± 28.48%
Δ MTV%	−37.83% ± 65.57%	−78.66% ± 452.34%	−18.26% ± 33.49%	−22.28% ± 48.53%
Δ TLG%	−7.59% ± 32.96%	−13.63% ± 101.84%	2.18% ± 19.64%	4.04% ± 20.02%

BPL, Bayesian penalty likelihood; MTV, metabolic tumor volume; SBR, signal-to-background ratio; SUV, standardized uptake value; TLG, total-lesion-glycolysis.

Fig. 3

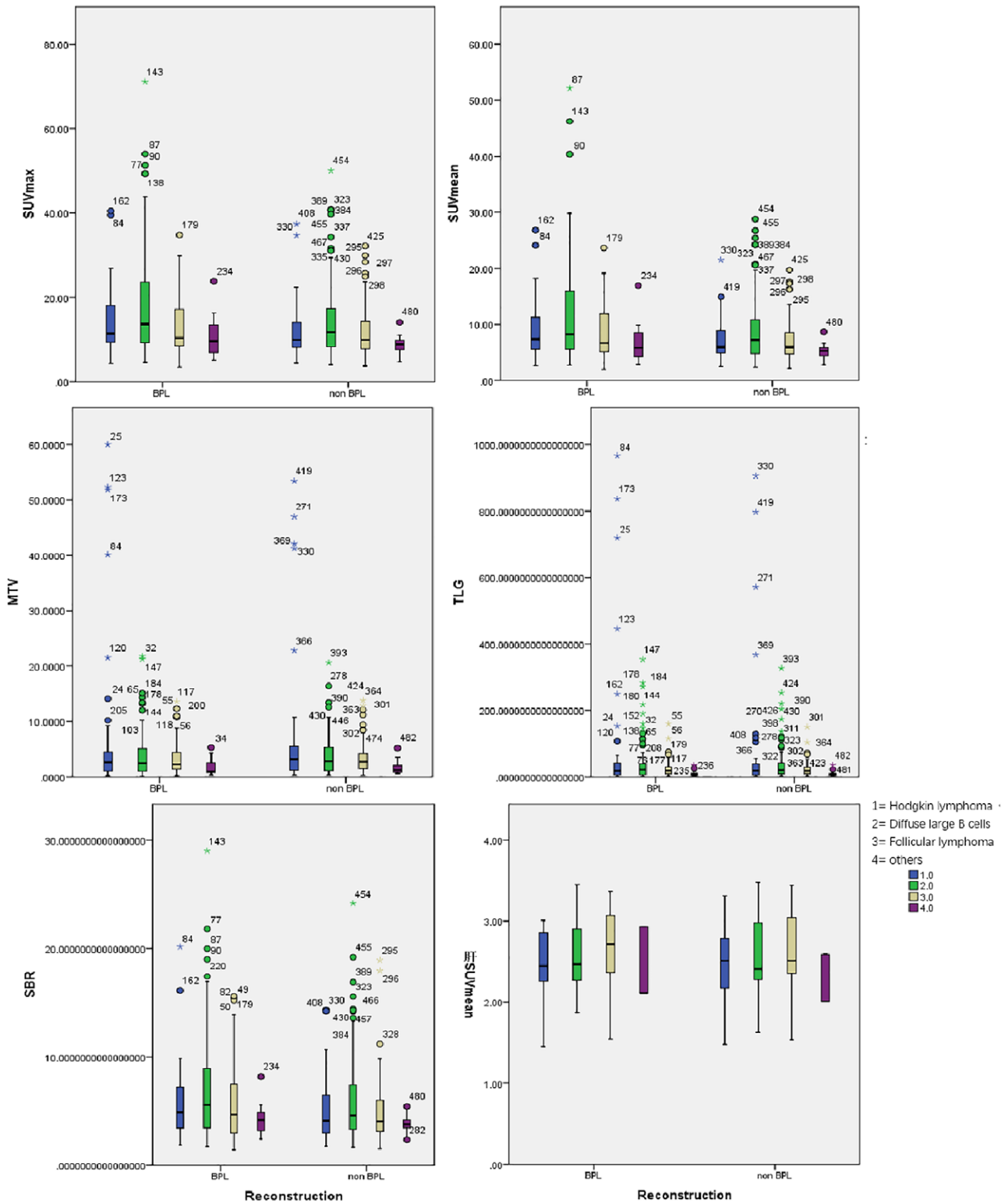


Diagram of metabolic parameters among different pathological groups.

Table 5 Comparison of metabolic parameters of different lesion sizes

Diameter	Parameter	Mean	SD	T	P-value
D < 1 cm	SUVmax	3.31	5.97	4.33	0.000
	SUVmean	1.72	1.82	9.00	0.000
	MTV	-0.39	0.73	-4.15	0.000
	Liver SUVmean	0.01	0.21	0.31	0.756
	TLG	-0.98	3.68	-2.09	0.041
	SBR	1.23	2.42	3.97	0.000
1 cm < D < 2 cm	SUVmax	2.27	4.50	6.05	0.000
	SUVmean	1.92	2.43	14.23	0.000
	MTV	-0.30	1.09	-3.31	0.001
	Liver SUVmean	0.01	0.17	0.99	0.326
	TLG	0.63	5.89	1.28	0.203
	SBR	0.87	2.00	5.24	00.000
D > 2 cm	SUVmax	0.92	3.05	1.96	0.057
	SUVmean	0.64	4.95	5.54	0.052
	MTV	0.85	2.95	1.87	0.069
	Liver SUVmean	-0.01	0.17	-0.57	0.572
	TLG	20.59	32.56	4.10	0.000
	SBR	0.37	2.25	1.05	0.298

MTV, metabolic tumor volume; SBR, signal-to-background ratio; SUV, standardized uptake value; TLG, total-lesion-glycolysis.

It has been confirmed that the new algorithm BPL had little effect on the liver background. Although the background noise in the liver was higher under PSF reconstruction [20] than BPL, generally TOF and PSF had little effect on the liver and mediastinal uptake [21]. In a clinical study of colorectal cancer liver metastasis [22], the BPL reconstruction algorithm improved the SNR and SBR of colorectal cancer liver metastasis detected by 18F-FDG-PET/CT and increased the lesion SUVmax without changing the background SUV or image noise of the liver. In the clinical application of lymphoma, PET/CT is often used in mid-treatment and post-chemotherapy evaluation, using the Deauville score (DeauvilleScore, DC) to distinguish between responders and nonresponders [23]. DC is a visual assessment criterion to classify the malignant/benign nature and to quantify the treatment response. The strongest uptake of lymphoma lesions was compared with the physiological uptake of mediastinal blood pool and liver (background) to evaluate the response to treatment. DS1–3 is defined as responder and DS4–5 is defined as nonresponders [1]. Because of the improvement of SBR, the BPL algorithm is more effective in the detection of medium and low background (such as mediastinal lymph nodes and pulmonary nodules). However, because it affects the value of SUVmax in small lesions [24], but does not significantly affect the background value, it may overestimate the overall tumor load, thus changing the classification of DS [25]. Enilorac *et al.* [26] recently studied whether the choice of reconstruction methods affected the DS. In their study of 126 patients, although different reconstruction methods led to changes in DS in a small number of patients, Kaplan–Meier analysis showed that there were statistical differences in progression-free survival and overall survival between responders and nonresponders,

no matter which reconstruction method was used for intertreatment and posttreatment PET imaging. It was suggested that the risk stratification of 18F-FDG-PET in patients with diffuse large B-cell lymphoma was not affected by the selective reconstruction algorithm, because the 2-y PSF and OS were similar. In another study [27], including all types of lymphoma, not just diffuse large B-cell lymphoma, they also found significant differences in DS classification in some patients with BPL algorithm and concluded that it needed further research to determine which reconstruction algorithm is better to evaluate the prognosis of lymphoma. In our study, the pathology of all lymphomas was included. The differences in liver background and SBR in other pathological groups may be due to the small sample size and small lesions in this group. In the subtypes of lymphoma with high FDG metabolisms, such as DLBCL, HL, and FL, the BPL algorithm had a significant effect on the SUVmax, SUVmean, and SBR of the lesions. Therefore, when comparing the DS scores of different centers, we still need to consider the consistency of the reconstruction algorithm.

In the past few years, PET was used as a routine in radiotherapy planning and clinical treatment response evaluation. At present, the traditional method is to measure the MTV of lesions according to the threshold. In this experiment, a 40% threshold was selected to determine the lesion volume. It was found that different pathologies had no obvious effect on MTV, but the size of lesions was related to the measurement of MTV. For lesions whose diameters were less than 2 cm, the BPL algorithm had a greater impact on MTV. This might be related to the PVE and the Gibbs artifact caused by BPL reconstruction [16]. In the BPL algorithm, there is no post-filtering processing, only by increasing the penalty factor β to generate a smoother image, so the relationship between MTV and β selection needs to be further studied. Moreover, MTV measurement could be affected by the contour algorithm [28]. Although there are other voxel-based threshold methods [29], which have a good advantage only for lesions with strong heterogeneity, and for areas with low contrast, the new contour algorithm may become unstable. More research on the impact of MTV will be carried out in the future. Many previous studies have reported PET semiquantitative parameters such as SUVmax or MTV as potential prognostic imaging markers in cancer patients [30,31]. Through effective complete convergence, the BPL reconstruction algorithm can represent more accurately these parameters in the future. Although the sample size of this retrospective study was not large enough, we have shown that, especially for small lesions, SBR has been significantly improved and lesion SUVmax has increased significantly, which may better assist in the clinical diagnosis of small lesions of lymphoma.

Acknowledgements

Conflicts of interest

There are no conflicts of interest.

Reference

- Barrington SF, Kluge R. FDG PET for therapy monitoring in Hodgkin and non-Hodgkin lymphomas. *Eur J Nucl Med Mol Imaging* 2017; **44**:97–110.
- Andre MP, Girinsky T, Federico M, Omumedaly R, Fortpied C, Gotti M, *et al.* Early positron emission tomography response-adapted treatment in stage I and II Hodgkin lymphoma: final results of the randomized EORTC/LYSA/FIL H10 trial. *J Clin Oncol* 2017; **35**:JCO2016686394.
- Lois C, Jakoby BW, Long MJ, Hubner KF, Barker DW, Casey ME, *et al.* An assessment of the impact of incorporating time-of-flight information into clinical PET/CT imaging. *J Nucl Med* 2010; **51**:237–245.
- Alessio AM, Stearns CW, Tong S, Ross SG, Kohlmyer S, Ganin A, Kinahan PE. Application and evaluation of a measured spatially variant system model for PET image reconstruction. *IEEE Trans Med Imaging* 2010; **29**:938–949.
- Akamatsu G, Mitsumoto K, Taniguchi T, Tsutsui Y, Baba S, Sasaki M. Influences of point-spread function and time-of-flight reconstructions on standardized uptake value of lymph node metastases in FDG-PET. *Eur J Radiol* 2014; **83**:226–230.
- GE Healthcare. PET/CT millennium specifics. http://www3.gehealthcare.co.uk/en-gb/products/categories/molecular_imaging/pet-ct/discovery_mi. [Accessed 21 November 2018].
- Ahn S, Ross SG, Asma E, Miao J, Jin X, Cheng L, *et al.* Quantitative comparison of OSEM and penalized likelihood image reconstruction using relative difference penalties for clinical PET. *Phys Med Biol* 2015; **60**:5733–5751.
- Reynés-Llompert G, Gámez-Cenzano C, Vercher-Conejero JL, Sabaté-Llobera A, Calvo-Malvar N, Martí-Climent JM. Phantom, clinical, and texture indices evaluation and optimization of a penalized-likelihood image reconstruction method (Q.Clear) on a BGO PET/CT scanner. *Med Phys* 2018; **45**:3214–3222.
- Teoh EJ, McGowan DR, Macpherson RE, Bradley KM, Gleeson FV. Phantom and clinical evaluation of the bayesian penalized likelihood reconstruction algorithm Q.Clear on an LYSO PET/CT system. *J Nucl Med* 2015; **56**:1447–1452.
- Van der Vos CS, Koopman D, Rijnsdorp S, Arends AJ, Boellaard R, Van Dalen JA, *et al.* Quantification, improvement, and harmonization of small lesion detection with state-of-the-art PET. *Eur J Nucl Med Mol Imaging* 2017; **44**:4–16.
- Conti M. Focus on time-of-flight PET: the benefits of improved time resolution. *Eur J Nucl Med Mol Imaging* 2011; **38**:1147–1157.
- Rapisarda E, Bettinardi V, Thielemans K, Gilardi MC. Image-based point spread function implementation in a fully 3D OSEM reconstruction algorithm for PET. *Phys Med Biol* 2010; **55**:4131–4151.
- Armstrong IS, Kelly MD, Williams HA, Matthews JC. Impact of point spread function modelling and time of flight on FDG uptake measurements in lung lesions using alternative filtering strategies. *EJNMMI Phys* 2014; **1**:99.
- Reynés-Llompert G, Gámez-Cenzano C, Romero-Zayas I, Rodríguez-Bel L, Vercher-Conejero JL, Martí-Climent JM. Performance characteristics of the whole-body discovery IQ PET/CT system. *J Nucl Med* 2017; **58**:1155–1161.
- Lindström E, Sundin A, Trampal C, Lindsjö L, Ilan E, Danfors T, *et al.* Evaluation of penalized-likelihood estimation reconstruction on a digital time-of-flight PET/CT scanner for 18F-FDG whole-body examinations. *J Nucl Med* 2018; **59**:1152–1158.
- Rogasch JM, Suleiman S, Hofheinz F, Bluemel S, Lukas M, Amthauer H, Furth C. Reconstructed spatial resolution and contrast recovery with Bayesian penalized likelihood reconstruction (Q.Clear) for FDG-PET compared to time-of-flight (TOF) with point spread function (PSF). *EJNMMI Phys* 2020; **7**:2.
- Kurita Y, Ichikawa Y, Nakanishi T, Tomita Y, Hasegawa D, Murashima S, *et al.* The value of Bayesian penalized likelihood reconstruction for improving lesion conspicuity of malignant lung tumors on 18F-FDG PET/CT: comparison with ordered subset expectation maximization reconstruction incorporating time-of-flight model and point spread function correction. *Ann Nucl Med* 2020; **34**:272–279.
- Howard BA, Morgan R, Thorpe MP, Turkington TG, Oldan J, James OG, Borges-Neto S. Comparison of Bayesian penalized likelihood reconstruction versus OS-EM for characterization of small pulmonary nodules in oncologic PET/CT. *Ann Nucl Med* 2017; **31**:623–628.
- Teoh EJ, McGowan DR, Bradley KM, Belcher E, Black E, Gleeson FV. Novel penalised likelihood reconstruction of PET in the assessment of histologically verified small pulmonary nodules. *Eur Radiol* 2016; **26**:576–584.
- Rahmim A, Qi J, Sossi V. Resolution modeling in PET imaging: theory, practice, benefits, and pitfalls. *Med Phys* 2013; **40**:064301.
- Aide N, Lasnon C, Veit-Haibach P, Sera T, Sattler B, Boellaard R. EANM/EARL harmonization strategies in PET quantification: from daily practice to multicentre oncological studies. *Eur J Nucl Med Mol Imaging* 2017; **44**:17–31.
- Parvizi N, Franklin JM, McGowan DR, Teoh EJ, Bradley KM, Gleeson FV. Does a novel penalized likelihood reconstruction of 18F-FDG PET-CT improve signal-to-background in colorectal liver metastases? *Eur J Radiol* 2015; **84**:1873–1878.
- Biggi A, Gallamini A, Chauvie S, Hutchings M, Kostakoglu L, Gregoriani M, *et al.* International validation study for interim PET in ABVD-treated, advanced-stage Hodgkin lymphoma: interpretation criteria and concordance rate among reviewers. *J Nucl Med* 2013; **54**:683–690.
- Hsu DFC, Ilan E, Peterson WT, Uribe J, Lubberink M, Levin CS. Studies of a next-generation silicon-photomultiplier-based time-of-flight PET/CT system. *J Nucl Med* 2017; **58**:1511–1518.
- Barrington SF, Sulkin T, Forbes A, Johnson PWM. All that glitters is not gold - new reconstruction methods using Deauville criteria for patient reporting. *Eur J Nucl Med Mol Imaging* 2018; **45**:316–317.
- Enilorac B, Lasnon C, Nganoa C, Fruchart C, Gac AC, Damaj G, Aide N. Does PET reconstruction method affect Deauville score in lymphoma patients? *J Nucl Med* 2018; **59**:1049–1055.
- Ly J, Minarik D, Edenbrandt L, Wollmer P, Trägårdh E. The use of a proposed updated EARL harmonization of 18F-FDG PET-CT in patients with lymphoma yields significant differences in Deauville score compared with current EARL recommendations. *EJNMMI Res* 2019; **9**:65.
- Zhuang M, Garcia DV, Kramer GM, Frings V, Smit EF, Dierckx R, *et al.* Variability and repeatability of quantitative uptake metrics in 18F-FDG PET/CT of non-small cell lung cancer: impact of segmentation method, uptake interval, and reconstruction protocol. *J Nucl Med* 2019; **60**:600–607.
- Hofheinz F, Langner J, Petr J, Beuthien-Baumann B, Steinbach J, Kotzerke J, van den Hoff J. An automatic method for accurate volume delineation of heterogeneous tumors in PET. *Med Phys* 2013; **40**:082503.
- Horne ZD, Clump DA, Vargo JA, Shah S, Berwal S, Burton S, *et al.* Pretreatment SUVmax predicts progression-free survival in early-stage non-small cell lung cancer treated with stereotactic body radiation therapy. *Radiat Oncol* 2014; **9**:41.
- Shim SH, Kim DY, Lee DY, Lee SW, Park JY, Lee JJ, *et al.* Metabolic tumour volume and total lesion glycolysis, measured using preoperative 18F-FDG PET/CT, predict the recurrence of endometrial cancer. *BJOG* 2014; **121**:1097–106.